

Passivity-based Dynamic Visual Force Feedback Control for Fixed Camera Systems

Hiroyuki Kawai, Toshiyuki Murao and Masayuki Fujita

Abstract—This paper investigates passivity based 3D dynamic visual force feedback control for fixed camera systems. In our approach, we can control not only the position but also the orientation of the robot hand with a contact force by using visual information. The proposed method can be regarded as an extension of the hybrid position/force control to the hybrid vision/force control. The main contribution of this paper is to show that the 3D dynamic visual force feedback system has the passivity which allows us to prove stability in the sense of Lyapunov. Both the passivity of the manipulator dynamics and the passivity of the visual feedback system are preserved. Finally simulation results on 3DOF planar manipulator are presented to verify the stability of the 3D dynamic visual force feedback system and understand our proposed method simply.

I. INTRODUCTION

Robotics and intelligent machines need sensory information to behave autonomously in dynamical environments. Visual information is particularly suited to recognize unknown surroundings. Vision based control of robotic systems involves the fusion of robot kinematics, dynamics, and computer vision to control the motion of the robot in an efficient manner. The combination of mechanical control with visual information, so-called visual feedback control or visual servoing, is important when we consider a mechanical system working under dynamical environments [1][2].

For the theoretically problem of three dimensional(3D) visual servo control based on the robot control theory, Kelly *et al.* [3] considered a simple image-based controller under the assumption that the objects' depths are known. Chen *et al.* [4] addressed the field-of-view problem for 3D dynamic visual feedback system using an image-space navigation function. In our previous works, we discussed the dynamic visual feedback control for 3D target tracking based on passivity [5][6]. On the other hand, applications of visual feedback system are also increasing in many fields. For example, recent applications of visual feedback system include the autonomous injection of biological cells [7], laparoscopic surgery [8] and others. Although visual information is necessary in order to recognize environments, only visual information is not enough to complete tasks in these applications. For example, not only visual information but also force information are needed to inject DNA to

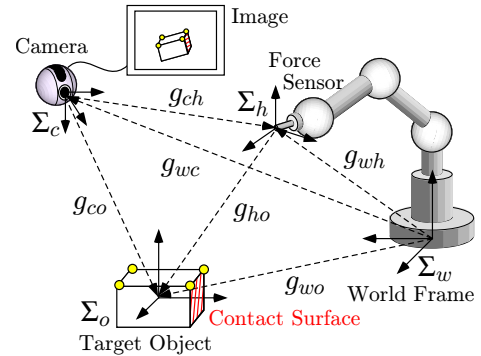


Fig. 1. Visual force feedback system with a fixed camera configuration.

biological cells. Hence, integrating visual feedback control with force control is important for the modern robot.

Xiao *et al.* [9] developed sensor fusion scheme for controlling an end-effector to follow an unknown trajectory on a contact surface. Baeten *et al.* [10] addressed a hybrid control structure for the eye-in-hand vision and force control. Although many practical methods are reported with experimental results, rigorous results have hardly been obtained in terms of the nonlinear control aspects. For this problem, Dean-León *et al.* [11] have combined image-based visual feedback control with force control and discussed the stability of the nonlinear system. The authors have proposed passivity based visual force feedback control law for force control with target tracking [12]. Although these control laws guarantee Lyapunov stability and are effective for the visual force feedback system, they are restricted to planar manipulators.

This paper deals with 3D visual force feedback control for fixed camera systems as depicted in Fig. 1. In our proposed method, we can control not only the position but also the orientation of the robot hand with a contact force in the visual force feedback system. The main contribution of this paper is to show that the 3D visual force feedback system has the passivity which allows us to prove stability in the sense of Lyapunov. Both the passivity of the manipulator dynamics and the passivity of the visual feedback system are preserved in the 3D visual force feedback system. Finally simulation results are shown to verify the stability of the proposed method.

II. VISUAL FEEDBACK SYSTEM

This section mainly reviews our previous works ([5], [6]) via the passivity based visual feedback control. Throughout

H. Kawai is with Department of Robotics, Kanazawa Institute of Technology, Ishikawa 921-8501, Japan hiroyuki@neptune.kanazawa-it.ac.jp
T. Murao is with Master Program of Information Systems Architecture, Advanced Institute of Industrial Technology, Tokyo 140-0011, Japan
M. Fujita is with Department of Mechanical and Control Engineering, Tokyo Institute of Technology, Tokyo 152-8550, Japan

this paper, we use the notation $e^{\hat{\xi}\theta_{ab}} \in \mathcal{R}^{3 \times 3}$ to represent the change of the principle axes of a frame Σ_b relative to a frame Σ_a . $\xi_{ab} \in \mathcal{R}^3$ specifies the direction of rotation and $\theta_{ab} \in \mathcal{R}$ is the angle of rotation. For simplicity we use $\hat{\xi}\theta_{ab}$ to denote $\hat{\xi}_{ab}\theta_{ab}$. The notation ‘ \wedge ’ (wedge) is the skew-symmetric operator such that $\hat{\xi}\theta = \xi \times \theta$ for the vector cross-product \times and any vector $\theta \in \mathcal{R}^3$. The notation ‘ \vee ’ (vee) denotes the inverse operator to ‘ \wedge ’, i.e., $so(3) \rightarrow \mathcal{R}^3$. Recall that a skew-symmetric matrix corresponds to an axis of rotation (via the mapping $a \mapsto \hat{a}$). We use the 4×4 matrix

$$g_{ab} = \begin{bmatrix} e^{\hat{\xi}\theta_{ab}} & p_{ab} \\ 0 & 1 \end{bmatrix} \quad (1)$$

as the homogeneous representation of $g_{ab} = (p_{ab}, e^{\hat{\xi}\theta_{ab}}) \in SE(3)$ describing the configuration of a frame Σ_b relative to a frame Σ_a . The adjoint transformation associated with g_{ab} is denoted by $\text{Ad}_{(g_{ab})}$ [14].

A. Basic Representation for Visual Feedback System

Visual feedback systems with a fixed camera configuration typically use four coordinate frames which consist of a world frame Σ_w , a target object frame Σ_o , a camera frame Σ_c and a hand (end-effector) frame Σ_h as in Fig. 1. Then, $g_{wh} = (p_{wh}, e^{\hat{\xi}\theta_{wh}}) \in SE(3)$, $g_{wc} = (p_{wc}, e^{\hat{\xi}\theta_{wc}}) \in SE(3)$ and $g_{wo} = (p_{wo}, e^{\hat{\xi}\theta_{wo}}) \in SE(3)$ denote the rigid body motion from Σ_w to Σ_h , from Σ_w to Σ_c and from Σ_w to Σ_o , respectively. Similarly, the relative rigid body motion from Σ_c to Σ_h , from Σ_c to Σ_o and from Σ_h to Σ_o can be represented by $g_{ch} = (p_{ch}, e^{\hat{\xi}\theta_{ch}}) \in SE(3)$, $g_{co} = (p_{co}, e^{\hat{\xi}\theta_{co}}) \in SE(3)$ and $g_{ho} = (p_{ho}, e^{\hat{\xi}\theta_{ho}}) \in SE(3)$, respectively, as shown in Fig. 1. The objective of the visual feedback control is to bring the actual relative rigid body motion g_{ho} to a given reference $g_d = (p_d, e^{\hat{\xi}\theta_d})$ which is constant in this paper. In other words, our goal is to determine the motion of hand by using the visual information.

The relative rigid body motion from Σ_c to Σ_o can be led by using the composition rule for rigid body transformations ([14], Chap. 2, pp. 37, eq. (2.24)) as follows:

$$g_{co} = g_{wc}^{-1} g_{wo}. \quad (2)$$

The relative rigid body motion involves the velocity of each rigid body. To this aid, let us consider the velocity of a rigid body as described in [14]. We define the body velocity of the camera relative to the world frame Σ_w as $V_{wc}^b = [v_{wc}^T \ \omega_{wc}^T]^T$, where v_{wc} and ω_{wc} represent the velocity of the origin and the angular velocity from Σ_w to Σ_c , respectively ([14] Chap. 2, eq. (2.55)).

Differentiating (2) with respect to time, the body velocity of the relative rigid body motion g_{co} can be written as follows (See [5]):

$$V_{co}^b = -\text{Ad}_{(g_{co}^{-1})} V_{wc}^b + V_{wo}^b \quad (3)$$

where V_{wo}^b is the body velocity of the target object relative to Σ_w . In the case of the fixed camera configuration, i.e. $V_{wc}^b =$

0, the model of the relative rigid body motion g_{co} can be rewritten as

$$V_{co}^b = V_{wo}^b. \quad (4)$$

Roughly speaking, if both the camera and the target object move, then the relative rigid body motion g_{co} will be derived from the difference between the camera velocity V_{wc}^b and the target object velocity V_{wo}^b . Hence, the model of the relative rigid body motion from Σ_c to Σ_o equals the target object velocity V_{wo}^b .

B. Estimation Error System

The relative rigid body motion g_{co} can not be immediately obtained in the visual feedback system, because the target object velocity is unknown and furthermore can not be measured directly. Hence, we consider the estimation problem of the relative rigid body motion g_{co} . The visual feedback control task requires information of the relative rigid body motion g_{co} . Since the measurable information is only the image information $f(g_{co})$ in the visual feedback system, we consider a nonlinear observer in order to estimate the relative rigid body motion g_{co} from the image information $f(g_{co})$.

Firstly, using the basic representation (4), we choose estimates \bar{g}_{co} and \bar{V}_{co}^b of the relative rigid body motion and velocity, respectively as

$$\bar{V}_{co}^b = u_e. \quad (5)$$

The new input u_e is to be determined in order to drive the estimated values \bar{g}_{co} and \bar{V}_{co}^b to their actual values.

In order to establish the estimation error system, we define the estimation error between the estimated value \bar{g}_{co} and the actual relative rigid body motion g_{co} as

$$g_{ee} = \bar{g}_{co}^{-1} g_{co}. \quad (6)$$

Using the notation $e_R(e^{\hat{\xi}\theta})$, the vector of the estimation error is defined as $e_e := [p_{ee}^T \ e_R^T(e^{\hat{\xi}\theta_{ee}})]^T$. Note that $e_e = 0$ iff $p_{ee} = 0$ and $e^{\hat{\xi}\theta_{ee}} = I_3$. Therefore, if the vector of the estimation error is equal to zero, then the estimated relative rigid body motion \bar{g}_{co} equals the actual relative rigid body motion g_{co} .

Suppose the attitude estimation error θ_{ee} is small enough that we can let $e^{\hat{\xi}\theta_{ee}} \simeq I + \text{sk}(e^{\hat{\xi}\theta_{ee}})$. Therefore, using a first-order Taylor expansion approximation, the estimation error vector e_e can be obtained from image information $f(g_{co})$ and the estimated value of the relative rigid body motion \bar{g}_{co} as follows [5]:

$$e_e = J^\dagger(\bar{g}_{co})(f - \bar{f}), \quad (7)$$

where \bar{f} is the estimated value of image information. In the same way as the basic representation (4), the estimation error system can be represented by

$$V_{ee}^b = -\text{Ad}_{(g_{ee}^{-1})} u_e + V_{wo}^b. \quad (8)$$

It should be noted that if the vector of the estimation error is equal to zero, then the estimated relative rigid body motion \bar{g}_{co} equals the actual one g_{co} .

C. Control Error Systems

In this subsection, let us consider the dual of the estimation error system, which we call the control error system, in order to establish the visual feedback system. We assume that g_{wc} and g_{wh} can be obtained accurately by a prior calibration procedure, then the estimated value of g_{ho} is calculated as $\bar{g}_{ho} = g_{ch}^{-1}\bar{g}_{co}$ where \bar{g}_{co} is the estimated value which discussed in the previous subsection. Here, we define the control error between the actual relative rigid body motion g_{ho} and desired one g_d as

$$g_{ec} = g_d^{-1}g_{ho}. \quad (9)$$

It should be noted that g_{ho} can not be measured directly. Similar to the definition of e_e , the vector of the control error is defined as $e_c := [p_{ec}^T \ e_R^T(e^{\hat{\xi}\theta_{ec}})]^T$.

Here we have to consider the way of deriving g_{ec} (9), because g_{ho} can not be measured directly. Using g_{ee} , the control error can be transformed as

$$g_{ec} = g_d^{-1}g_{ho} = g_d^{-1}\bar{g}_{ho}^{-1}\bar{g}_{ho}g_{ho} = g_d^{-1}\bar{g}_{ho}^{-1}g_{ee}. \quad (10)$$

In Equation (10), g_d and \bar{g}_{ho} While the estimation error vector e_e can be obtained as Equation (7), the estimation error matrix g_{ee} cannot be directly obtained, because g_{ee} is defined using non-measurable value g_{co} as Equation (6). Therefore, we consider the way of deriving g_{ee} from e_e .

Because of the definition of the estimation error vector e_e , i.e., $e_e := [p_{ee}^T \ e_R^T(e^{\hat{\xi}\theta_{ee}})]^T$, the position estimation error p_{ee} can be derived directly from e_e . Under the condition $-\frac{\pi}{2} \leq \theta_{ee} \leq \frac{\pi}{2}$, $\xi\theta_{ee}$ can be derived as follows [6]:

$$\xi\theta_{ee} = \frac{\sin^{-1} \|e_R(e^{\hat{\xi}\theta_{ee}})\|}{\|e_R(e^{\hat{\xi}\theta_{ee}})\|} e_R(e^{\hat{\xi}\theta_{ee}}). \quad (11)$$

Hence, g_{ee} can be derived from e_e through $\xi\theta_{ee}$.

The reference of the relative rigid body motion g_d is constant in this paper, i.e., $\dot{g}_d = 0$, hence, $V_{ec}^b = V_{ho}^b$. Thus, the control error system can be represented as

$$V_{ec}^b = -\text{Ad}_{(g_{ec}^{-1})}\text{Ad}_{(g_d^{-1})}V_{wh}^b + V_{wo}^b. \quad (12)$$

This is dual to the estimation error system.

D. Passivity of Visual Feedback System

Combining (8) and (12), we construct the visual feedback system as follows:

$$\begin{bmatrix} V_{ec}^b \\ V_{ee}^b \end{bmatrix} = \begin{bmatrix} -\text{Ad}_{(g_{ec}^{-1})} & 0 \\ 0 & -\text{Ad}_{(g_{ee}^{-1})} \end{bmatrix} u_{ce} + \begin{bmatrix} I \\ I \end{bmatrix} V_{wo}^b \quad (13)$$

where $u_{ce} := [(\text{Ad}_{(g_d^{-1})}V_{wh}^b)^T \ u_e^T]^T$ denotes the control input. For the design of the visual feedback system, it is assumed that the hand velocity V_{wh}^b can be directly chosen. Let us define the error vector of the visual feedback system as $e := [e_c^T \ e_e^T]^T$ which consists of the control error vector e_c and the estimation error vector e_e .

Next, we show an important relation between the input and the output of the visual feedback system.

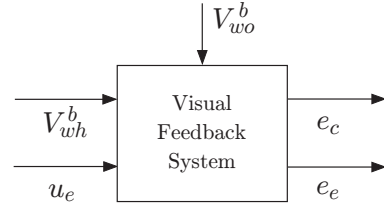


Fig. 2. Block diagram of the visual feedback system.

Lemma 1: [5] If $V_{wo}^b = 0$, then the visual feedback system (13) satisfies

$$\int_0^T u_{ce}^T \nu_{ce} dt \geq -\beta_{ce}, \quad \forall T > 0 \quad (14)$$

where ν_{ce} is defined as $\nu_{ce} := -e$ and β_{ce} is a positive scalar.

Using the following positive definite function, we can prove Lemma 1.

$$V_{ce} = E(g_{ec}) + E(g_{ee}) \quad (15)$$

where $E(g_{ab}) := \frac{1}{2}\|p_{ab}\|^2 + \phi(e^{\hat{\xi}\theta_{ab}})$ and $\phi(e^{\hat{\xi}\theta_{ab}}) := \frac{1}{2}\text{tr}(I - e^{\hat{\xi}\theta_{ab}})$ is the error function of the rotation matrix (see, e.g., [13]).

The block diagram of the passivity of the visual feedback system is shown in Fig. 2. Let us take u_{ce} as the input and ν_{ce} as its output in Fig. 2. Thus, Lemma 1 implies that the visual feedback system (13) is *passive* from the input u_{ce} to the output ν_{ce} as in the definition in [15].

III. DYNAMIC VISUAL FORCE FEEDBACK CONTROL

A. Dynamic Visual Force Feedback System

The dynamics of n -link rigid robot manipulators with the end-effector constraint can be written as follows [16]

$$M(q)\ddot{q} + C(q, \dot{q})\dot{q} + g(q) = \tau + J_\varphi(q)\lambda \quad (16)$$

where q , \dot{q} and \ddot{q} are the joint angle, velocity and acceleration, respectively, τ is the vector of the input torque. $M(q) \in \mathcal{R}^{n \times n}$ is the manipulator inertia matrix, $C(q, \dot{q}) \in \mathcal{R}^{n \times n}$ is the Coriolis matrix and $g(q) \in \mathcal{R}^n$ is the gravity vector. $\lambda \in \mathcal{R}$ is the contact force, $J_\varphi(q) \in \mathcal{R}^n$ is the normalized Jacobian of the kinematic constraint $\varphi(q) = 0 \in \mathcal{R}$ and defined as follows.

$$J_\varphi^T(q)\dot{q} = 0, \quad J_\varphi(q) = \left[\frac{\partial \varphi(q)}{\partial q} \right]^T \in \mathcal{R}^n \quad (17)$$

Equation (16) possesses several important properties which will be used in the sequel. The manipulator dynamics (16) is passive from τ to \dot{q} , that is $\int_0^T \tau^T \dot{q} dt \geq -\beta_m$ where β_m is a positive scalar. Moreover, $M(q) - 2C(q, \dot{q})$ is skew-symmetric by defining $C(q, \dot{q})$ using the Christoffel symbols.

Now, we propose the control law for the manipulator as

$$\begin{aligned} \tau = & M(q)\ddot{q}_r + C(q, \dot{q})\dot{q}_r + g(q) \\ & + J_b^T(q)\text{Ad}_{(g_d^{-1})}^T e_c - J_\varphi \lambda_d + u_s + J_\varphi u_F \end{aligned} \quad (18)$$

where

$$\dot{q}_r := Q_\varphi(q)\dot{q}_d + \alpha J_\varphi(q)F_e. \quad (19)$$

α is positive constant and

$$F_e := \int_0^t (\lambda - \lambda_d)d\tau = \int_0^t e_\lambda d\tau \in \mathcal{R} \quad (20)$$

where $e_\lambda := \lambda - \lambda_d$ is the force error. Then, the following relation holds with respect to about the force error

$$\dot{F}_e = e_\lambda. \quad (21)$$

Because we consider the single point contact in this paper, the projection matrix $Q_\varphi(q)$ can be simply defined as

$$Q_\varphi(q) = I - J_\varphi(q)J_\varphi^T(q) \quad (22)$$

which arises on the tangent space at the contact surface $\varphi(q) = 0$ [16].

On the other hand, the body velocity of the hand V_{wh}^b is given by

$$V_{wh}^b = J_b(q)\dot{q} \quad (23)$$

where $J_b(q)$ is the body manipulator Jacobian [14]. Moreover, we design the reference of the joint velocity as

$$\dot{q}_d := Q_\varphi^\dagger(q) \left(J_b^\dagger(q)u_h - \alpha J_\varphi(q)F_e \right) \quad (24)$$

where $u_h = [v_{uh}^T \ \omega_{uh}^T]^T$ is the desired body velocity of the hand which will be obtained from the visual feedback system.

We define the error vector with respect to the joint velocity of the manipulator dynamics as

$$s := \dot{q} - \dot{q}_r \in \mathcal{R}^n \quad (25)$$

Here, we know that the following relation holds [16]

$$J_\varphi^T s = -\alpha F_e. \quad (26)$$

Using (13)(16) and (18), the visual force feedback system with manipulator dynamics (we call the dynamic visual force feedback system) can be derived as follows:

$$\begin{bmatrix} \dot{s} \\ \dot{F}_e \\ V_{ec}^b \\ V_{ee}^b \end{bmatrix} = \begin{bmatrix} -M^{-1} \left(Cs - J_b^T \text{Ad}_{(g_d^{-1})}^T e_c - J_\varphi e_\lambda \right) \\ e_\lambda \\ -\text{Ad}_{(g_{ho}^{-1})} J_b s \\ 0 \end{bmatrix} + \begin{bmatrix} M^{-1} & M^{-1}J_\varphi & 0 & 0 \\ 0 & 0 & 0 & 0 \\ 0 & 0 & -\text{Ad}_{(g_{ec}^{-1})} & 0 \\ 0 & 0 & 0 & -\text{Ad}_{(g_{ee}^{-1})} \end{bmatrix} u + \begin{bmatrix} 0 \\ 0 \\ I \\ I \end{bmatrix} w \quad (27)$$

where

$$x := \begin{bmatrix} s \\ F_e \\ e_c \\ e_e \end{bmatrix} \quad u := \begin{bmatrix} u_s \\ u_F \\ \text{Ad}_{(g_d^{-1})} u_c \\ u_e \end{bmatrix} \quad w := V_{wo}^b,$$

are defined as the state, the input and the disturbance of the dynamic visual force feedback system, respectively. Here, we formulate the manipulator control problem as follows:

Control problem : For the dynamic visual force feedback system with the fixed camera configuration described by (27), design a control input u such that

$$\lim_{t \rightarrow \infty} s = 0, \quad \lim_{t \rightarrow \infty} F_e = 0, \quad \lim_{t \rightarrow \infty} e_c = 0 \quad \text{and} \quad \lim_{t \rightarrow \infty} e_e = 0.$$

B. Passivity of Dynamic Visual Force Feedback System

Before constructing the dynamic visual force feedback control law, we derive an important lemma.

Lemma 2: If $w = 0$, then the dynamic visual force feedback system (27) satisfies

$$\int_0^T u^T \nu \geq -\beta, \quad \forall T > 0 \quad (28)$$

where $\nu := Nx$, $N := \text{diag}\{I_n, -\alpha, -I_6, -I_6\}$ and β is a positive scalar.

Proof: Consider the following positive definite function

$$V = \frac{1}{2} s^T M s + \frac{1}{2} \alpha F_e^2 + E(g_{ec}) + E(g_{ee}). \quad (29)$$

Differentiating (29) with respect to time yields

$$\begin{aligned} \dot{V} &= s^T M \dot{s} + \frac{1}{2} s^T \dot{M} s + \alpha F_e \dot{F}_e \\ &\quad + p_{ec}^T e^{\hat{\xi}\theta_{ec}} e^{-\hat{\xi}\theta_{ec}} \dot{p}_{ec} + e_R^T (e^{\hat{\xi}\theta_{ec}}) e^{\hat{\xi}\theta_{ec}} \omega_{ec} \\ &\quad + p_{ee}^T e^{\hat{\xi}\theta_{ee}} e^{-\hat{\xi}\theta_{ee}} \dot{p}_{ee} + e_R^T (e^{\hat{\xi}\theta_{ee}}) e^{\hat{\xi}\theta_{ee}} \omega_{ee} \\ &= x^T \begin{bmatrix} M & 0 & 0 & 0 \\ 0 & \alpha & 0 & 0 \\ 0 & 0 & \text{Ad}_{(e^{\hat{\xi}\theta_{ec}})} & 0 \\ 0 & 0 & 0 & \text{Ad}_{(e^{\hat{\xi}\theta_{ee}})} \end{bmatrix} \begin{bmatrix} \dot{s} \\ \dot{F}_e \\ V_{ec}^b \\ V_{ee}^b \end{bmatrix} + \frac{1}{2} s^T \dot{M} s. \end{aligned} \quad (30)$$

Observing that the skew-symmetry of the matrices \hat{p}_{ec} and \hat{p}_{ee} , i.e., $p_{ec}^T \hat{p}_{ec} e^{-\hat{\xi}\theta_d} \omega_{ud} = -p_{ec}^T (e^{-\hat{\xi}\theta_d} \omega_{ud})^\wedge p_{ec} = 0$, $p_{ee}^T \hat{p}_{ee} \omega_{ue} = -p_{ee}^T \hat{\omega}_{ue} p_{ee} = 0$, the above equation along the trajectories of the system (27) can be transformed into

$$\begin{aligned} \dot{V} &= -s^T C \dot{s} + s^T J_b^T \text{Ad}_{(g_d^{-1})}^T e_c + s^T J_\varphi e_\lambda + \alpha F_e e_\lambda \\ &\quad - e_c^T \text{Ad}_{(g_{ho}^{-1})} J_b s + \frac{1}{2} s^T \dot{M} s \\ &\quad + x^T \begin{bmatrix} M & 0 & 0 & 0 \\ 0 & \alpha & 0 & 0 \\ 0 & 0 & \text{Ad}_{(e^{\hat{\xi}\theta_{ec}})} & 0 \\ 0 & 0 & 0 & \text{Ad}_{(e^{\hat{\xi}\theta_{ee}})} \end{bmatrix} \\ &\quad \times \begin{bmatrix} M^{-1} & M^{-1}J_\varphi & 0 & 0 \\ 0 & 0 & 0 & 0 \\ 0 & 0 & -\text{Ad}_{(g_{ec}^{-1})} & 0 \\ 0 & 0 & 0 & -\text{Ad}_{(g_{ee}^{-1})} \end{bmatrix} u \\ &= \frac{1}{2} s^T (\dot{M} - 2C) s + e_\lambda^T (J_\varphi s + \alpha F_e) + x^T N^T u \\ &= x^T N^T u. \end{aligned} \quad (31)$$

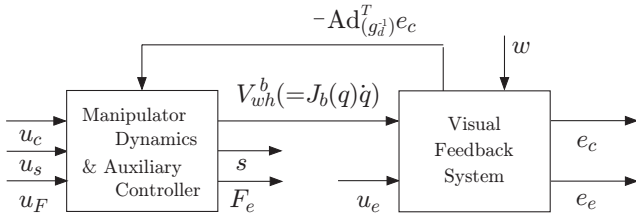


Fig. 3. Block diagram of the 3D dynamic visual force feedback system.

Integrating (31) from 0 to T , we obtain

$$\int_0^T u^T \nu d\tau = V(T) - V(0) \geq -V(0) = -\beta \quad (32)$$

where β is a positive scalar that only depends on the initial states of s , F_e , e_c and e_e . ■

The block diagram of the passivity of the 3D dynamic visual force feedback system is shown in Fig. 3.

Remark 1: The visual feedback system (13) satisfies the passivity property as described in (14). It is well known that the manipulator dynamics (16) also has the passivity. In Lemma 2, the inequality (28) says that the dynamic visual force feedback system (27) is *passive* from the input $u = [u_s^T \ u_F^T \ (\text{Ad}_{(g^{-1})} u_c)^T \ u_e^T]^T$ to the output $\nu = [s^T \ -\alpha F_e^T \ -e_c^T \ -e_e^T]^T$ as shown in Fig. 3.

C. Passivity-based Dynamic Visual Force Feedback Control

We now propose the following control input for the interconnected system:

$$u = -K\nu = -KNx \quad (33)$$

$$K := \text{diag}\{K_s, k_F, K_c, K_e\} \in \mathcal{R}^{n+13}$$

where $K_s := \text{diag}\{k_{s1}, \dots, k_{sn}\}$, k_F , $K_c := \text{diag}\{k_{c1}, \dots, k_{c6}\}$ and $K_e := \text{diag}\{k_{e1}, \dots, k_{e6}\}$ denote the positive gain matrices.

Theorem 1: If $w = 0$, then the equilibrium point $x = 0$ for the closed-loop system (27) and (33) is asymptotic stable.

Proof: In the proof of Lemma 2, we have already derived that the time derivative of V along the trajectory of the system (27) is formulated as (31). Using the control input (33), (31) can be transformed into

$$\dot{V} = -x^T N^T K N x. \quad (34)$$

This completes the proof. ■

Theorem 1 shows the stability via Lyapunov method for the dynamic visual force feedback system. It is interesting to note that stability analysis is based on the passivity as described in (28). Our proposed method is valid for the 3D dynamic visual force feedback system, while previous works [11][12] consider the 2D dynamic visual force feedback control. Hence, we can control not only the position but also the orientation of the robot hand with a contact force in the visual force feedback system.

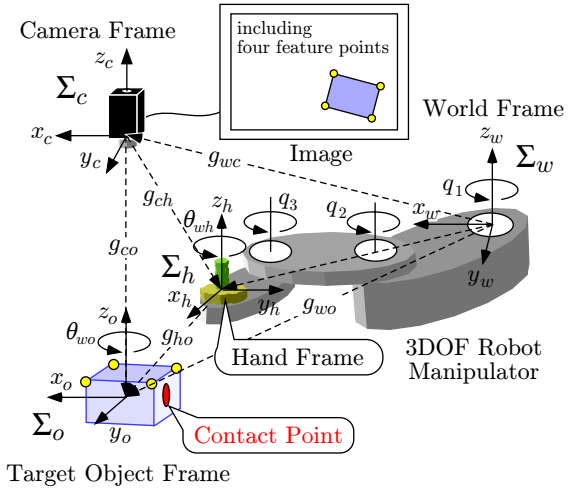


Fig. 4. Coordinate frames for dynamic visual force feedback system with three degree of freedom manipulator.

IV. SIMULATION RESULTS

The simulation results on 3DOF planar manipulator as depicted in Fig. 4 are shown in order to understand our proposed method simply, though it is valid for 3D dynamic visual force feedback systems.

We present results for the stability analysis with a static target object. The simulation is carried out with the conditions $p_{wo} = [0.47 \ 0.05 \ 0]^T$ [m], $\xi_{\theta_{wo}} = [0 \ 0 \ 0]^T$ [rad], $p_{wc} = [0.47 \ 0.05 \ 1]^T$ [m], $\xi_{\theta_{wc}} = [0 \ 0 \ 0]^T$ [rad]. The lengths of the three links of the manipulator are $l_1 = 0.2$ [m], $l_2 = 0.2$ [m] and $l_3 = 0.1$ [m], respectively. The initial angles of the manipulator is set as $q_1(0) = -\pi/2$ [rad], $q_2(0) = \pi/2$ [rad] and $q_3(0) = \pi/2$ [rad]. In other words, the initial relative rigid body motion is $p_{ho} = [0.15 \ -0.27 \ 0]^T$ [m], $\xi_{\theta_{ho}} = [0 \ 0 \ -\pi/2]^T$ [rad]. The desired force λ_d and the desired relative rigid body motion $g_d = (p_d, e^{\xi_{\theta_d}})$ are given by $\lambda_d = 5$ [N], $p_d = [0.03 \ 0 \ 0]^T$ [m] and $\xi_{\theta_d} = [0 \ 0 \ 0]^T$ [rad] in this simulation. The initial errors of force and vision are calculated as $\lambda_e = -5$ [N], $p_{ec} = [0.12 \ -0.27 \ 0]^T$ [m], $\xi_{\theta_{ec}} = [0 \ 0 \ -\pi/2]^T$ [rad], $p_{ee} = [0.53 \ 0.95 \ 0]^T$ [m] and $\xi_{\theta_{ee}} = [0 \ 0 \ \pi/4]^T$ [rad], respectively.

The controller parameters for Equation (33) were empirically selected as $K_s = \text{diag}\{10, 10, 10\}$, $k_F = 25$, $\alpha = 1$, $K_c = \text{diag}\{40, 40, 20, 20, 20, 40\}$ and $K_e = 50I_6$. The simulation results are shown in Figs. 5 and 7. Figs. 5–7 illustrate the control error e_c , the estimation error e_e , and the contact force λ , respectively. In Figs. 5 and 6, we focus on the errors of the translations of x and y and the rotation of z , because the errors of the translation of z and the rotations of x and y are zeros ideally on the 3DOF planar manipulator. The control error e_c and the estimation error e_e tended to zero, thus we can confirm that the relative rigid body motion g_{ho} coincided with the desired one g_d by using image information. In Fig. 7, the pulse signal means the contact transition at around 0.2 [s]. The contact force λ tended to 5 [N], i.e., converged to the desired one λ_d . From these figures, the asymptotic stability can be also confirmed.

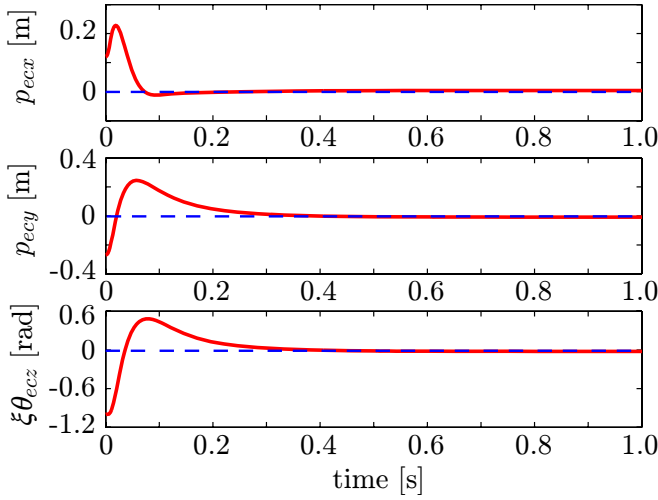


Fig. 5. The control error e_c which defined the error between the relative rigid body motion of the robot hand g_{ho} and desired one g_d . Initial control errors are $p_{ee_x} = 0.12$ [m], $p_{ee_y} = -0.27$ [m] and $\xi\theta_{ee_z} = -\pi/2$ [rad], respectively

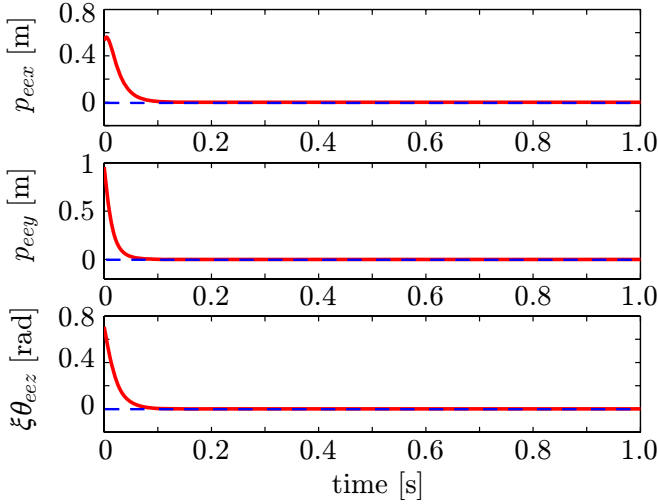


Fig. 6. The estimation error e_e which defined the error between the estimated value \bar{g}_{co} and the actual relative rigid body motion g_{co} . Initial estimation errors are $p_{ee_x} = 0.53$ [m], $p_{ee_y} = -0.95$ [m] and $\xi\theta_{ee_z} = \pi/4$ [rad], respectively

V. CONCLUSIONS

This paper considers 3D visual force feedback control for fixed camera systems. In our approach, we can control not only the position but also the orientation of the robot hand with a contact force by using visual information. The proposed method can be regarded as an extension of the hybrid position/force control to the hybrid vision/force control. The main contribution of this paper is to show that the visual force feedback system has the passivity which allows us to prove stability in the sense of Lyapunov. Both the passivity of the manipulator dynamics and the passivity of the visual feedback system are preserved in the visual force feedback system. Finally simulation results are shown to verify the stability of the proposed method.

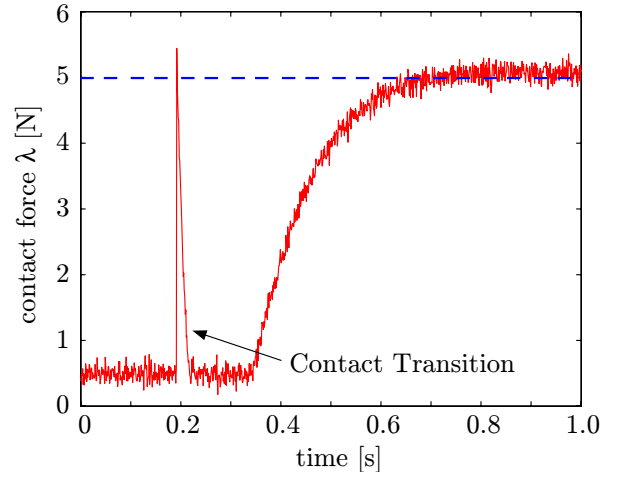


Fig. 7. The contact force trajectory λ .

REFERENCES

- [1] F. Chaumette and S. Hutchinson, "Visual Servo Control, Part I: Basic Approaches," *IEEE Robotics & Automation Magazine*, Vol. 13, No. 4, pp. 82–90, 2006.
- [2] F. Chaumette and S. Hutchinson, "Visual Servo Control, Part II: Advanced Approaches," *IEEE Robotics & Automation Magazine*, Vol. 14, No. 1, pp. 109–117, 2007.
- [3] R. Kelly, R. Carelli, O. Nasisi, B. Kuchen and F. Reyes, "Stable Visual Servoing of Camera-in-Hand Robotic Systems," *IEEE Trans. Mechatronics*, Vol. 5, No. 1, pp. 39–48, 2000.
- [4] J. Chen, D. M. Dawson, W. E. Dixon and V. K. Chitrakaran, "Navigation Function-based Visual Servo Control," *Automatica*, Vol. 43, No. 7, pp. 1165–1177, 2007.
- [5] M. Fujita, H. Kawai and M. Spong, "Passivity-based Dynamic Visual Feedback Control for Three Dimensional Target Tracking: Stability and L_2 -gain Performance Analysis," *IEEE Transactions on Control Systems Technology*, Vol. 15, No. 1, pp. 40–52, 2007.
- [6] T. Murao, H. Kawai and M. Fujita "Predictive Visual Feedback Control with Eye-in/to-Hand Configuration via Stabilizing Receding Horizon Approach," *Proc. of the 17th IFAC World Congress on Automatic Control*, 2008(to appear).
- [7] S. Yu and B. J. Nelson, "Autonomous Injection of Biological Cells Using Visual Servoing," In: D. Rus and S. Singh (Eds), *Experimental Robotics VII*, Springer-Verlag, pp. 169–178, 2001.
- [8] K. Omote *et al.*, "Self-Guided Robotic Camera Control for Laparoscopic Surgery Compared with Human Camera Control," *The American Journal of Surgery*, Vol. 177, No. 4, pp. 321–324, 1999.
- [9] D. Xiao, B. K. Ghosh, N. Xi and T. J. Tarn, "Sensor-based Hybrid Position/Force Control of a Robot Manipulator in an Uncalibrated Environment," *IEEE Transactions on Control Systems Technology*, Vol. 8, No. 4, pp. 635–645, 2000.
- [10] J. Baeten, H. Bruyninckx and J. D. Schutter, "Integrated Vision/Force Robotic Servoing in the Task Frame Formalism," *International Journal of Robotics Research*, Vol. 22, No. 10–11, pp. 941–954, 2003.
- [11] E.C. Dean-León, V. Parra-Vega and A. Espinosa-Romero, "Visual Servoing for Constrained Planar Robots Subject to Complex Friction," *IEEE/ASME Trans. on Mechatronics*, Vol. 11, No. 4, pp. 389–400, 2006.
- [12] H. Kawai, T. Murao and M. Fujita, "Passivity-based Visual Force Feedback Control for Planar Manipulators with Eye-in-Hand Configuration," *Proc. of 16th IEEE International Conference on Control Applications* pp. 1480-1485, 2007.
- [13] F. Bullo and A.D. Lewis, *Geometric Control of Mechanical Systems*, Springer-Verlag, 2004.
- [14] R. Murray, Z. Li and S. S. Sastry, *A Mathematical Introduction to Robotic Manipulation*, CRC Press, 1994.
- [15] A. van der Schaft, *L_2 -Gain and Passivity Techniques in Nonlinear Control* (2nd ed.), Springer-Verlag, 2000.
- [16] Y. Liu, K. Kitagaki, T. Ogasawara and S. Arimoto, "Model-based Adaptive Hybrid Control for Manipulators Under Multiple Geometric Constraints," *IEEE Trans. on Control Systems Technology*, Vol. 7, No. 1, pp. 97–109, 1999.